

# **Effects of ketamine on GABAergic and glutamatergic activity in the mPFC: biphasic recruitment of GABA function in antidepressant-like responses**

Manoela V. Fogaça<sup>1,2\*</sup>, Fernanda Daher<sup>1</sup> and Marina R. Picciotto<sup>2</sup>

<sup>1</sup> Department of Pharmacology and Physiology, University of Rochester Medical Center, 601 Elmwood Avenue, Rochester, NY 14642, USA

<sup>2</sup> Department of Psychiatry, Yale University School of Medicine, 34 Park Street, New Haven, CT 06519, USA

\* Corresponding author:

Manoela V. Fogaça, 601 Elmwood Avenue, Rochester, NY 14642, USA

manoela\_fogaca@urmc.rochester.edu

Phone: +1 (585) 273-5631

Running title: Biphasic recruitment of GABA activity in ketamine's actions

## 2 **Abstract**

3 Major depressive disorder (MDD) is associated with disruptions in glutamatergic and  
4 GABAergic activity in the medial prefrontal cortex (mPFC), leading to altered synaptic  
5 formation and function. Low doses of ketamine rapidly rescue these deficits, inducing fast and  
6 sustained antidepressant effects. While it is suggested that ketamine produces a rapid  
7 glutamatergic enhancement in the mPFC, the temporal dynamics and the involvement of GABA  
8 interneurons in its sustained effects remain unclear. Using simultaneous photometry recordings  
9 of calcium activity in mPFC pyramidal and GABA neurons, as well as chemogenetic approaches  
10 in *Gad1-Cre* mice, we explored the hypothesis that initial effects of ketamine on glutamate  
11 signaling trigger subsequent enhancement of GABAergic responses, contributing to its sustained  
12 antidepressant responses. Calcium recordings revealed a biphasic effect of ketamine on activity  
13 of mPFC GABA neurons, characterized by an initial transient decrease (phase 1, <30 min)  
14 followed by an increase (phase 2, >60 min), in parallel with a transient increase in  
15 excitation/inhibition levels (10 min) and lasting enhancement of glutamatergic activity (30-120  
16 min). Previous administration of ketamine enhanced GABA neuron activity during the sucrose  
17 splash test (SUST) and novelty suppressed feeding test (NSFT), 24 h and 72 h post-treatment,  
18 respectively. Chemogenetic inhibition of GABA interneurons during the surge of GABAergic  
19 activity (phase 2), or immediately before the SUST or NSFT, occluded ketamine's behavioral  
20 actions. These results indicate that time-dependent modulation of GABAergic activity is required  
21 for the sustained antidepressant-like responses induced by ketamine, suggesting that approaches  
22 to enhance GABAergic plasticity and function are promising therapeutic targets for  
23 antidepressant development.

24

25 **Keywords:** glutamate, GABA, mPFC, ketamine, depression, antidepressants, stress, plasticity

26

## 27 **Introduction**

28           Major depressive disorder (MDD) is a recurring neuropsychiatric illness that has a  
29 lifetime prevalence of ~17% in the U.S., and is a leading cause of disability worldwide (1).  
30 Despite the significant economic and human impact, the effectiveness of treatments remains  
31 suboptimal, underscoring MDD's inherent heterogeneity and our limited comprehension of the  
32 molecular and functional mechanisms that underlie its etiology (2). Traditional antidepressants  
33 take weeks to months to induce a therapeutic response, and up to 33% of patients prescribed  
34 these medications are considered treatment resistant (3). Conversely, low doses of ketamine, an  
35 NMDA receptor (NMDA-R) blocker, can induce rapid (2 h) and sustained (up to 7 days)  
36 antidepressant effects in patients diagnosed with MDD, even in patients that are refractory to  
37 current antidepressant medications (4).

38           Human and rodent studies indicate that depression and chronic stress are linked to  
39 structural alterations in limbic brain areas, including the medial prefrontal cortex (mPFC),  
40 characterized by reduced volume, neuronal atrophy, and impaired excitatory synapse density and  
41 function (5-9). Conversely, accumulating evidence suggests that ketamine can reverse these  
42 deficits and produce rapid antidepressant effects through an initial, transient blockade of NMDA  
43 receptors (NMDA-R) in GABA interneurons, leading fast disinhibition of excitatory pyramidal  
44 neurons and triggering neuronal plasticity in the mPFC (10-12). An alternative hypothesis is that  
45 ketamine acts directly on pyramidal neurons to block NMDA-R activity driven by spontaneous  
46 glutamate release (13).

47           Furthermore, in addition to disruption in excitatory synapses, MDD subjects and animals  
48 exposed to chronic stress have reductions in cortical and plasma GABA levels, as well as several  
49 GABA markers in the PFC (10, 14-20). Since inhibitory inputs control network excitability,

50 integration, and synchrony, deficits in GABA function compromise the signal-to-noise properties  
51 of glutamatergic neurons and the integrity of circuit-level information transmission from the  
52 mPFC to projection areas (5). Consistent with this idea, prefrontal cortical GABA abnormalities  
53 are associated with hippocampal structural deficits in MDD subjects (9) and normalization of  
54 GABA function is associated with remission of depressive symptoms (18, 21-27). Indeed,  
55 following the initial enhancement of glutamate function, ketamine and other rapid  
56 antidepressants also increase GABA signaling in the mPFC, potentially contributing to  
57 reestablishing the integrity of excitatory and inhibitory signal efficiency and precision in  
58 corticolimbic circuits (14-16, 19, 20, 28).

59 In this study, we hypothesized that ketamine might induce long-lasting changes in the  
60 activity of GABA interneurons that could contribute to sustained antidepressant effects. To test  
61 this, we imaged activity of mPFC pyramidal and GABA neurons simultaneously following  
62 ketamine administration and during behavioral tests relevant to antidepressant efficacy. We then  
63 employed chemogenetic approaches to investigate whether activity of GABA interneurons is  
64 necessary and/or required for the behavioral actions of ketamine.

65

## 66 **Materials and Methods**

### 67 *Animals*

68 Male glutamic acid decarboxylase 1 (*Gad1*)-*Cre* transgenic mice and WT littermates (8-12-  
69 week-old) on the C57BL/6 background were bred in-house as in previous studies (29, 30).  
70 Male mice were initially chosen to allow for comparison of the outcomes observed following  
71 ketamine administration with previous literature, predominantly described in male mice. All  
72 animals were group-housed with a 12/12h light-dark cycle and food and water *ad libitum*.  
73 Following surgery for viral infusion and/or optical fiber placement, animals were single housed  
74 for 4 weeks and remained isolated until the end of the experiments. All procedures were  
75 conducted in compliance with the National Institute of Health (NIH) guidelines for the care and  
76 use of laboratory animals and were approved by the Yale Institutional Animal Care and Use  
77 Committee.

78

### 79 *Viral constructs and surgery*

80 Adeno-associated viruses AAV.CamKII.GCaMP6s.WPRE.SV40, pAAV.Syn.Flex.NES-  
81 jRCaMP1b.WPRE.SV40,  $\geq 1 \times 10^{13}$  vg/ml, and AAV2-hSyn-DIO-hM4D(Gi)-mCherry  
82 (hM4DGi),  $\geq 7 \times 10^{12}$  vg/ml, were obtained from Addgene (USA). To image activity of  
83 pyramidal neurons and GABA interneurons simultaneously, anesthetized *Gad1-Cre* mice  
84 (ketamine, 100 mg/kg; and xylazine, 10 mg/kg) received unilateral intra-mPFC infusion of a  
85 cocktail (1:1; 0.6  $\mu$ l, 0.1 $\mu$ l/min) containing two calcium sensors with non-overlapping spectra:  
86 CaMKII-driven GCaMP6s (GCaMP6s) and Cre-driven jRCaMP1b (RCaMP) viruses  
87 (coordinates from bregma: anterior-posterior: +1.9 mm; medial-lateral:  $\pm$  0.4 mm; dorsal-ventral  
88 -2.7 mm), along with implantation of a fiber (stainless steel ferrule, 400  $\mu$ m core, 0.50 NA, 2.5

89 mm length, ThorLabs, Newton, New Jersey, USA) in the same region. The fiber was implanted  
90 0.2 mm above the injection site and maintained in place with adhesive dental cement (C&B-  
91 Metabond, Parkell, NY, USA). Animals received i.p. injections of carprofen (5 mg/kg)  
92 immediately after the surgery and daily for the next 2 days. Following surgery, all animals  
93 remained single-housed throughout the duration of the protocols. In this study, single housing  
94 was used to prevent detachment of the optical fiber from the skull and to serve as a chronic mild  
95 stressor to study inhibitory and excitatory neuronal activity. To preserve the integrity of the  
96 cannula, including a control group not subjected to isolation, which would enable comparing  
97 stress effects, was not feasible for practical reasons. For chemogenetic experiments, animals  
98 received bilateral infusion of inhibitory hM4DGi (0.5  $\mu$ l/side; 0.1 $\mu$ l/min) into the mPFC and  
99 underwent the same post-surgery protocol as described, including single housing. Fiber  
100 placement and viral efficiency were analyzed using a confocal microscope to obtain Z-stack  
101 image sequences (Leica TSE-SPE) (30).

102

### 103 *Drug administration*

104 Ketamine (Sigma-Aldrich, 10 mg/kg, i.p.) was dissolved in saline. Clozapine-N-oxide (CNO, 0.5  
105 or 1 mg/kg i.p., Enzo Life Sciences, Farmingdale, NY, USA) was administered at different time  
106 points, as indicated, based on our previous studies indicating lack of behavioral and locomotor  
107 effects at these low doses (30); however, to control for any off target effects that have been  
108 reported at higher doses (5-10 mg/kg) (31, 32), both WT and *Gad1-Cre* groups received CNO.

109

### 110 *Behavioral studies*

111 Animals were habituated to testing rooms 30 min before each experiment. All behavioral tests  
112 were video recorded and conducted between 10 a.m. and 4 p.m. Experiments were scored by an  
113 experimenter blind to treatments.

114 *Sucrose Splash Test (SUST)*: A 10% sucrose solution was squirted onto the dorsal coat of the  
115 mouse, as has been described (33). Grooming time was measured for 5 min.

116 *Novelty-Suppressed Feeding Test (NSFT)*: Mice were food deprived for 16 h and placed in a  
117 dimly lit box (40 x 40 x 25) with a pellet of food in the center; the latency to feed was measured  
118 with a time limit of 10 min, as described (30). Immediately after the test, home cage food intake  
119 was measured over a 10 min period as a feeding control.

120

#### 121 *Immunofluorescence*

122 *Gad-Cre* mice received a Cre-dependent hM4DGi viral infusion into the mPFC, as described,  
123 and SST or PV co-localization with Gad-hM4DGi<sup>+</sup> cells was assessed using primary antibodies  
124 (mouse anti-SST #sc-74556, 1:200, Santa Cruz; rabbit anti-PV #ab181086, 1:1000, Abcam) and  
125 appropriate secondary antibodies (AlexaFluor® 488 goat anti-rabbit or AlexaFluor® 647 goat  
126 anti-mouse, 1:1000), as described (20, 30). For quantification, sections containing the mPFC  
127 were analyzed using a Keyence BZ-X800 microscope equipped with an optical sectioning  
128 module (20X magnification). The total number of Gad-hM4DGi<sup>+</sup>, PV or SST neurons, as well as  
129 Gad-hM4DGi<sup>+</sup> co-localized with PV<sup>+</sup> or SST<sup>+</sup> cells, were obtained within each section (3  
130 sections/animal). The results were then averaged across animals (n = 3 mice) and expressed as a  
131 percentage of co-localized cells (number of co-localized Gad-hM4DGi<sup>+</sup> and SST or PV  
132 cells/total Gad-hM4DGi<sup>+</sup>, PV or SST cells × 100).

133

134 *Fiber photometry*

135 Multichannel fluorescent signals were recorded with a Tucker RZ5P processor (Tucker-Davis  
136 Technologies, Alachua, FL, USA) controlled by the Synapse software suite to display excitation  
137 (465 nm for GCaMP, green, and 560 nm for RCaMP, red) and reference (405 nm, isobestic  
138 control) signals, modulated at 531, 330 and 211 Hz, respectively. The LEDs (Doric, Quebec,  
139 Canada) were adjusted to the photodetector (Newport 2151, Irvine, CA, USA) with excitation  
140 light intensity of  $\sim 20 \mu\text{W}$ . Light was passed through a minicube (FMC6AE, Doric) that  
141 contained excitation and emission filter sets. Animals were tethered to the system via fiber optic  
142 patch cord (400  $\mu\text{M}$  core, 0.50 NA, ThorLabs) connected to a head mounted fiber optic cannula  
143 via a ceramic sleeve.

144

145 *Data processing and analysis*

146 Signals were low pass filtered with a frequency cutoff of 5 Hz using MATLAB. The excitation  
147 signal for each channel was analyzed using an adaptive iteratively reweighted Penalized Least  
148 Squares (airPLS) algorithm to correct bleaching and motion artifacts, and regressed against the  
149 reference control signal, using the protocol developed by Martianova et al., 2019 (34) (available  
150 at [https://github.com/katemartian/Photometry\\_data\\_processing](https://github.com/katemartian/Photometry_data_processing)). The change in fluorescence  
151 ( $dF/F$ ) was calculated as  $dF/F$  (465 nm or 560 nm signal–fitted 405-nm signal)/fitted 405-nm  
152 signal. To standardize signals across animals prior to analysis, results were normalized by z-  
153 scoring and expressed as average z-scored  $dF/F$ . As it is currently not possible to use an isobestic  
154 point for red-shifted sensors (RCaMP), the 405 nm signal was used as a reference for correcting  
155 movement artifacts, as described (34). However, due to the nature of photobleaching associated  
156 with long-term recordings shown in Figure 1 ( $\sim 150$  min), RCaMP fluorescence intensity



157 displayed a gradually decreasing trend evident in the vehicle-treated group (Supplementary  
158 Figure 1). Therefore, bleaching in this experiment was additionally corrected applying the  
159 Matlab linear function *detrend* ( $y = \text{detrend}(x, n)$ , where  $n = 1$ ;  $x - y = \text{linear trend}$ ) to the  
160 vehicle-treated group, and the resultant curve was subtracted from saline and ketamine signals,  
161 as described (35). The *detrend* algorithm computes the least-squares fit of a straight line (or  
162 composite line for piecewise linear trends) to the data and subtracts the resulting function from  
163 the data. For this correction, we assumed that saline had no significant effects on calcium  
164 fluorescence over time. Detrending was not required for the shorter recordings described in  
165 Figures 2 and 3 (up to 60 min). To evaluate excitation/inhibition levels, baseline or 10-min  
166 binned data were transformed into positive values by adding a constant, and the ratio of GCaMP  
167 to RCaMP transients ( $dF/F$ ) was calculated within each animal.

168 In the behavioral studies, z-scores of each epochs of interest (e.g., time blocks following  
169 ketamine treatment and during behavioral tests, and the bite event) were averaged across groups  
170 and presented in bar graphs. In the NSFT, to account for variability in the time it takes for  
171 different animals to bite the food (e.g., to remove a chunk of food from the pellet), the bite event  
172 was defined as a 5-second period encompassing the food interaction and bite.

173

#### 174 *Statistical analysis*

175 Results were subjected to repeated measures ANOVA (treatment  $\times$  time) with Sidak's correction  
176 for multiple analyses. Additionally, Student's two-tailed t-test or Two-way ANOVA (treatment  $\times$   
177 genotype) followed by Duncan test were employed as appropriate. All distributions were tested  
178 for homogeneity of variance using Levene's test and for normality using the Kolmogorov-  
179 Smirnov test. Non-normal distributions were analyzed by Mann-Whitney U test (two-tailed) or

180 Friedman's two-way analysis of variances by ranks test. Sphericity was assessed by Mauchly's  
181 test. In cases where the assumption of sphericity was violated, the data were analyzed using the  
182 Greenhouse-Geisser correction. Across all analyses, differences were considered significant at  $p$   
183  $\leq 0.05$ . Sample sizes were chosen based on previous experience with the tests employed and  
184 power analyses (Cohen's  $d$  power analysis,  $> 0.8$  effect size) conducted following a pilot study.  
185 For all analyses, we used the SPSS Software (v 29.0) or GraphPrism (v 9.5.1). The specific test  
186 used for each experiment is described in the figure legend. Each experiment was replicated a  
187 minimum of 2 times.

188

## 189 **Results**

190 *Photometry recordings immediately after treatment: ketamine enhances activity of excitatory*  
191 *mPFC neurons and elicits a biphasic response in GABAergic neurons*

192 The rapid antidepressant actions of ketamine are thought to involve initial inhibition of GABA  
193 interneurons, leading to a subsequent glutamate burst and enhancement of glutamatergic activity  
194 in the mPFC (12, 30). Additionally, ketamine administration increases GABA-related synaptic  
195 proteins in the mPFC 24 h post-administration (20). However, the temporal dynamics of  
196 excitatory and inhibitory neuronal activity in the mPFC following ketamine administration has  
197 not been measured. To address this, we infused CaMKII-driven GCaMP6s (green) and Cre-  
198 driven jRCaMP1b (RCaMP, red) viruses into the mPFC of *Gad1-Cre* mice to record calcium  
199 activity from both glutamatergic (CaMKII<sup>+</sup>) and GABAergic (Gad<sup>+</sup>) neurons simultaneously  
200 (Figure 1A). Although previous studies indicate that the CaMKII promoter can lead to unspecific  
201 expression in inhibitory neurons (36, 37), our analysis suggest no significant overlap (Figure

202 1B). Using this dual-channel strategy, we observed that ketamine administration increases the  
203 activity of CaMKII<sup>+</sup> neurons beginning approximately 30 min after administration, and this  
204 response persists until the end of the recording period (120 min, Figure 1C, F). In contrast,  
205 ketamine decreases the activity of GABA neurons for the first 30 min after administration  
206 compared to the vehicle-treated group. It is noteworthy that, since the injection procedure  
207 initially produced some level of GABA activity evident in the vehicle-treated group during the  
208 first 10 min post-injection (Supplementary Figure 2B), the reduction in calcium transients  
209 produced by ketamine becomes apparent only when compared with the vehicle group but not  
210 with the baseline (Figure 1D). This response is inverted after 60 min, such that there is a delayed  
211 increase in GABA activity compared to baseline (60 min) and to the baseline and vehicle-treated  
212 groups (90-120 min) (Figure 1D, G). Finally, because GABAergic and glutamatergic activity  
213 shift in opposite directions immediately after ketamine treatment (Supplementary Figure 2), we  
214 conducted further analysis to investigate the initial dynamics of ketamine's actions on E/I levels  
215 within each animal. Given that ketamine reaches peak plasma and brain levels within 10 min of  
216 intraperitoneal administration in mice (38), we assessed E/I activity during baseline and within  
217 10 or 20 min post-treatment. Interestingly, our results revealed a rapid and transient increase in  
218 E/I transients following ketamine administration (10 min) in comparison to its baseline and the  
219 vehicle-treated group, which returned to baseline levels shortly thereafter (Figure 1E). These data  
220 show that ketamine triggers a biphasic response in GABA interneurons, characterized by a  
221 transient decrease followed by an increase of activity.

222

223 *Ketamine enhances activity of mPFC pyramidal and GABAergic neurons 24 h post-treatment*  
224 *during the sucrose splash test*

225 Next, we investigated whether ketamine-induced rapid changes in glutamatergic and GABAergic  
226 activity are long-lasting and engaged during stress-relevant behavioral tests. An independent  
227 cohort of *Gad1-Cre* mice underwent surgery for virus infusion, along with implantation of an  
228 optical fiber, as outlined. Twenty-four hours after vehicle or ketamine treatment, animals  
229 underwent recording in the home cage to evaluate sustained effects of ketamine in the absence of  
230 behavioral challenge (50 min, Supplementary Figure 3) and then during the SUST (5 min)  
231 (Figure 2A). Ketamine administration did not alter baseline activity of GABAergic or  
232 glutamatergic neurons 24 h after administration (50-min recording, Supplementary Figure 3A-  
233 B). For visualization and statistical analyses, baseline traces in Figure 2 represent the last 300 sec  
234 of baseline recordings. Ketamine increased grooming time during the SUST (300 sec) (Figure  
235 2B), and increased calcium transients in both glutamatergic (Figure 2C, E-F) and GABAergic  
236 cells (Figure 2D, E, G) in comparison to respective baselines and vehicle-treated groups.

237  
238 *Ketamine enhances activity of GABAergic neurons 72 h post-treatment during the novelty*  
239 *suppressed feeding test*

240 Animals then underwent recordings 72 h following ketamine treatment to evaluate  
241 calcium transients in the home cage (50 min) and during the NSFT (10 min) (Figure 3A). As  
242 expected, ketamine decreased the latency to feed in the NSFT 72 h following treatment  
243 compared to the vehicle-treated group (Figure 3B). No change was observed in the home cage  
244 food consumption (Supplementary Figure 4). The results indicate that ketamine did not alter  
245 baseline activity of GABAergic or glutamatergic neurons 72 h after administration (0-50 min)  
246 (Supplementary Figure 4A-B). For visualization and statistical analyses, baseline traces in Figure  
247 3 represent the last 300 sec of baseline recordings. During the NSFT, ketamine administration

248 led to a strong trend towards increased calcium activity in glutamatergic cells compared to the  
249 baseline condition, although it did not reach statistical significance ( $p = 0.06$ , Figure 3C).  
250 Conversely, there was an increase in calcium transients in GABAergic neurons during the NSFT  
251 in both vehicle- and ketamine-treated groups compared to the respective baseline groups (Figure  
252 3F). However, ketamine produced a more robust increase in GABAergic activity during the first  
253 150 s of test duration compared to the vehicle-treated group (Figure 3F). We also measured the  
254 average z-scored  $dF/F$  paired specifically to the bite event (Figure 3D and G). Interestingly, these  
255 results show that ketamine treatment results in activation of GABA interneurons but not  
256 pyramidal neurons during the bite event, suggesting that ketamine-induced plasticity in  
257 GABAergic neurons is long-lasting and manifest during an avoidance-related behavioral task.

258

259 *Chemogenetic inhibition of mPFC GABA neurons following ketamine treatment or during*  
260 *behavioral tests at 24 h or 72 h occludes ketamine's behavioral actions*

261 Based on the biphasic GABAergic activity observed after ketamine treatment (Figure 1),  
262 characterized by an initial decrease (phase 1) followed by an increase (phase 2) in calcium  
263 transients, we sought to investigate whether this delayed enhancement of GABA function is  
264 required for the sustained behavioral responses induced by ketamine. To address this, *Gad1-Cre*  
265 and WT littermate controls were infused bilaterally with a Cre-dependent hM4DGi virus (Figure  
266 4A-B) to selectively inhibit the activity of GABA interneurons in the mPFC during phase 2. To  
267 investigate whether the hM4DGi virus expression is restricted to specific subpopulations of  
268 interneurons or encompasses overall GABAergic cells in *Gad-Cre* mice, we conducted  
269 immunostaining to co-label *Gad*- hM4DGi<sup>+</sup> cells with PV or SST. Our results indicate that  
270 30.7% of the *Gad*- hM4DGi<sup>+</sup> cells express SST, while 27.1% express PV, revealing

271 heterogeneity within the *Gad-Cre* line (Figure 4C; Supplementary Figure 5). Although PV is  
272 shown to be more expressed than SST in the neocortex (40% vs 30%, respectively) (39), most of  
273 our injections are confined to layers II/III and, to a lesser extent, V of the mPFC, where PV and  
274 SST cells are shown to be similarly expressed (39). Conversely, 18.1% and 25.6% of total  
275 labeled PV or SST cells, respectively, were Gad- hM4DG<sup>+</sup>.

276 In this experimental setup, animals received either vehicle or ketamine (10 mg/kg),  
277 followed by CNO (1 mg/kg) 40 min later (Figure 4A). This schedule of administration allows the  
278 initial ketamine-induced blockade of GABA interneurons to occur (<30 min, phase 1), while  
279 occluding the subsequent enhancement of GABA activity (phase 2). CNO has a short half-life in  
280 mice (~1 h) (31), so an additional low dose of CNO (0.5 mg/kg) was administered after 2 h to  
281 extend the effect. It is noteworthy that these low doses of CNO do not elicit behavioral or  
282 locomotor responses 24 h or 72 h later when injected in hM4DG<sup>+</sup>-infused *Gad1-Cre* mice (30).  
283 Ketamine increased grooming time in the SUST (24 h) and decreased the latency to feed in  
284 NSFT (72 h) in WT mice, as expected, and these effects were blocked by chemogenetic  
285 inhibition of GABA interneurons during phase 2 in *Gad1-Cre* mice (Figure 4D-E). No changes  
286 were observed in home cage food consumption (Figure 4D). This suggests that activity at  
287 GABAergic synapses is required for the sustained antidepressant-like effects of ketamine. In a  
288 separate control experiment, we adopted an inverse approach where hM4DG<sup>+</sup>-infused *Gad1-Cre*  
289 mice received CNO (1 mg/kg) 40 min *before* vehicle or ketamine, and then were tested in the  
290 SUST or NSFT, 24 or 72 h post-treatment, respectively (Supplementary Figure 6). This protocol  
291 allows us to evaluate CNO pre-treatment on ketamine's actions without affecting the delayed  
292 GABAergic surge, as CNO would be largely eliminated by this time. As expected, prior CNO  
293 treatment did not impact ketamine's behavioral effects in both the SUST (Supplementary Figure

294 6C) and NSFT (Supplementary Figure 6D), supporting our hypothesis that ketamine-induced  
295 GABAergic activity is time-dependent and engaged at a later timepoint.

296         Based on the observation that GABAergic transients are increased *during* the SUST and  
297 NSFT tests 24 and 72 h following ketamine treatment, respectively (Figure 2 and 3), we  
298 determined whether activation of GABA interneurons *during* these tests is required for the  
299 behavioral outcomes induced by ketamine. WT and *Gad1-Cre* mice were administered either  
300 vehicle or ketamine, followed by CNO (1 mg/kg) 24 and 72 h later, injected 30 min before each  
301 behavioral test (Figure 4F). Importantly, CNO does not produce any behavioral or locomotor  
302 effects when administered 30 min before behavioral tests in hM4DGi-infused *Gad1-Cre* mice  
303 (30). Previous ketamine administration increased grooming time in the SUST (24 h after  
304 administration) and decreased the latency to feed in NSFT (72 h after administration) in WT  
305 mice, and these effects were occluded by chemogenetic inhibition of GABA interneurons 30 min  
306 before each test (Figure 4G-H). No differences were observed in home cage food consumption  
307 among groups (Figure 4H). This suggests that ketamine-induced activity of GABAergic neurons  
308 is long-lasting and engaged during stress-related behavioral tasks.

309

## 310 **Discussion**

311 In this study we provide direct evidence that ketamine exerts sustained antidepressant-like  
312 actions through facilitation of GABA function. The results support the hypothesis that ketamine  
313 modulates the activity of mPFC GABA interneurons in a biphasic manner, with an initial  
314 decrease in activity (phase 1), accompanied by activation of pyramidal neurons, followed by an  
315 increase in GABA function (phase 2) (Figure 5). Notably, chemogenetic data indicate that this  
316 delayed enhancement of mPFC GABA activity is both required and necessary for the sustained

317 behavioral actions of ketamine. The increase in GABA signaling after ketamine administration is  
318 also long-lasting and engaged during behavioral tests relevant to stress responses, suggesting it  
319 may be involved in fine-tuning cortical circuits during stress-related behaviors.

320 A major hypothesis for the initial cellular trigger for ketamine's action is that it first  
321 blocks NMDA-R expressed by cortical interneurons, notably, somatostatin (SST) and  
322 parvalbumin (PV) GABA neuron subtypes (5, 12). Because these inhibitory neurons exhibit  
323 tonic firing, they are thought to be more sensitive to NMDA-R blockade, as tonic activity  
324 removes the  $Mg^{2+}$  block of the receptor, enabling ketamine to enter the channel pore and block  
325  $Ca^{2+}$  entry (12, 40). Inhibition of GABAergic interneuron firing decreases GABA activity,  
326 resulting in disinhibition of excitatory pyramidal neurons, and leading to a glutamate burst that  
327 drives activity-dependent BDNF release, activation of protein synthesis (via the mTORC1  
328 pathway), new spine formation, and synaptogenesis (2). Supporting this hypothesis, NMDA-R  
329 blockade leads to a reduction in the spontaneous firing of putative GABA interneurons in the  
330 mPFC, coupled with an enhanced activity of pyramidal neurons at a delayed rate (40).  
331 Furthermore, a low concentration of ketamine (1  $\mu M$ ), which approximates brain levels after *in*  
332 *vivo* administration, rapidly decreases inhibitory- and increases excitatory postsynaptic currents  
333 (IPSCs and EPSCs, respectively) onto pyramidal neurons in mPFC slices (12).

334 In this study we measured the dynamics in cellular responses to ketamine using  
335 simultaneous dual photometry recordings of GABA neurons and glutamatergic cells in the  
336 mPFC. Our findings indicate that ketamine initially produces a decrease in GABAergic neuron  
337 activity compared to the vehicle group, and a transient increase in E/I levels (10 min), followed  
338 by a long-lasting increase in pyramidal neuron activity (2 h). However, it remains unknown  
339 whether the initial decrease in GABAergic transients directly lead to enhanced glutamatergic



340 activity, and more studies addressing cross-correlational dynamics and causality are needed. In a  
341 previous study, increased GCaMP6f fluorescence in mPFC pyramidal neurons was observed 30  
342 min after administering a lower dose of ketamine (3 mg/kg), and this study reported more  
343 pronounced effects at 30 mg/kg, leading to an immediate increase in pyramidal activity lasting  
344 up to 20 min post-injection (41). However, it is noteworthy that the interpretation of that study is  
345 limited due to the absence of a vehicle control group. Selective knockdown of a key NMDA-R  
346 subunit, GluN2B, in GABA interneurons, but not pyramidal (CaMKII<sup>+</sup>) cells, occluded the  
347 behavioral actions of ketamine (12). Optogenetic stimulation of GABA interneurons concurrent  
348 with ketamine administration also occluded its behavioral effects (20). Similar cellular  
349 mechanisms are observed with other rapid antidepressant candidates, including the muscarinic  
350 acetylcholine receptor antagonist scopolamine (14, 29, 30). Stimulating GABA interneuron  
351 activity before scopolamine administration blocks its rapid and sustained behavioral effects (30).  
352 Likewise, selective knockdown or knockout of muscarinic type 1 (M1) receptors in SST  
353 interneurons occludes scopolamine-induced behavioral responses and molecular plasticity at  
354 GABAergic and glutamatergic synapses (14, 29). In the same direction, our previous studies  
355 have shown that chemogenetic inhibition of either all GAD-positive neurons in the mPFC, or  
356 only SST or PV interneuron subtypes, using a higher dose of CNO (2.5 mg/kg, 3x), resulted in  
357 fast antidepressant-like responses and molecular changes, mimicking the effects of fast  
358 antidepressants (30). Conversely, lower doses of CNO used in the present study (0.5 and 1  
359 mg/kg) are not sufficient to produce behavioral effects on their own, suggesting that a more  
360 robust silencing of GAD-positive neurons is required to recapitulate rapid antidepressant actions.

361 Interestingly, after the initial decrease in GABA activity, we observed a delayed  
362 enhancement of GABA function starting 60 min post-ketamine administration, which was further

363 engaged during behavioral tests 24 h and 72 h later, suggesting that additional mechanisms  
364 beyond glutamate-mediated plasticity might contribute to ketamine's actions (Figure 5). Indeed,  
365 our chemogenetic experiments provided evidence supporting the involvement of GABAergic  
366 interneurons in mediating the effects of ketamine. Notably, while the glutamatergic hypothesis  
367 provides a conceptual model for the rapid changes produced by ketamine, it does not account for  
368 the reductions in GABA levels and markers observed in cortical areas of human subjects with  
369 MDD and chronically stressed animals, which can be restored by rapid antidepressant treatment  
370 (10, 15-20, 28, 42-47). Several studies have reported decreases in the expression of SST and  
371 proteins related to GABA signaling, such as GAD1—the primary enzyme responsible for  
372 synthesizing GABA from glutamate—and multiple subunits of GABA<sub>A</sub> receptors in cortical  
373 tissues obtained from both MDD subjects and stressed animals (48-51). Mice lacking SST (SST-  
374 KO) exhibit increased stress-related behaviors, and reduced GAD1 gene expression (52).  
375 Importantly, normalization of cortical and plasma GABA levels, as well as GAD1 expression,  
376 following antidepressant treatment, is associated with remission of depressive symptoms (21-27).

377 Consistent with these findings, the antidepressant effects of ketamine are accompanied by  
378 robust increase in GABA levels in the mPFC of patients diagnosed with MDD or obsessive-  
379 compulsive disorder (19, 53). Ketamine can also restore impaired GABA release in the  
380 hippocampus of stressed rats (54). Our previous findings suggest that ketamine and other fast-  
381 acting drugs, including scopolamine, increase pre- and postsynaptic markers of GABA signaling  
382 in the mPFC 24 h after administration, such as GAD1, the vesicular GABA transporter (VGAT)  
383 and/or gephyrin, along with serotonin-induced IPSCs in pyramidal neurons (20). Ketamine can  
384 also modulate GABA<sub>A</sub>-R binding in human PFC and increase the activity of extrasynaptic  
385 GABA<sub>A</sub>-R in mouse cortex and hippocampus (55, 56). Combined administration of sub-effective

386 doses of muscimol, a selective agonist of GABA<sub>A</sub> receptors, and ketamine, produces  
387 antidepressant-like effects in mice (57). Global deletion or mutation of  $\gamma$ 2-GABA-R produces  
388 stress-induced phenotypes, which are reversed by a single dose of ketamine or chronic  
389 imipramine treatment (58). Ketamine also reverses GABAergic deficits in these animals,  
390 increasing inhibitory postsynaptic currents (IPSCs) and gephyrin levels (58). Additionally,  
391 disinhibition of somatostatin interneurons by deletion of  $\gamma$ 2-GABA-R selectively from these cells  
392 results in anxiolytic- and antidepressant-like effects, and confers resilience to stress in male  
393 mice, mimicking the effects of ketamine (59, 60). It is worth noting that the experiments in the  
394 present study were conducted in single-housed animals that underwent surgeries for cannula  
395 placement and/or viral infusion. Social isolation in rodents has been shown to disrupt  
396 corticolimbic structures and immune system function, contributing to stress-related behavioral  
397 outcomes (61-63). Thus, the single housing may have contributed to baseline stress in these mice  
398 that allowed robust changes in response to ketamine administration. However, further  
399 experiments using well-validated animal models of stress, such as the CUS, are necessary to  
400 evaluate the actions of ketamine compared to a control group (non-stressed).

401 While the precise mechanism by which ketamine enhances GABA activity remains  
402 unclear, one hypothesis is that, following the glutamatergic burst, there is homeostatic self-  
403 tuning adaptations to reestablish E/I balance in the mPFC (10). This local reorganization could  
404 restore the integrity of signal transfer to target regions by re-establishing correct firing patterns,  
405 and thereby promoting antidepressant effects (64) (Figure 5). Glutamate is the primary precursor  
406 of GABA as a substrate for GAD, so strengthened inhibition may be a self-limiting mechanism  
407 to prevent excitotoxicity in response to excessive excitation. Notably, activation of postsynaptic  
408 NMDA-R or stimulation of glutamatergic neurons (CaMKII<sup>+</sup>) engages a positive feedback

409 mechanism culminating in long-term potentiation of dendritic inhibition mediated by SST  
410 interneurons in the mPFC (65). Concomitantly, disrupting the glutamate-glutamine cycle  
411 depletes GABA neurotransmitter pools (66, 67), restoring balance through decreased inhibition.  
412 Another possibility is that ketamine exerts direct effects on the GABAergic system, potentially  
413 through its metabolites such as (2R, 6R)-HNK, which has shown ketamine-like antidepressant  
414 effects without prompting psychotomimetic responses (38, 68).

415 Our findings also reveal enhancement of glutamate neuron activity 24 h post-ketamine  
416 during the SUST; however, although there was a strong trend towards increased overall  
417 glutamatergic activity 72 h later during the NSFT, no effect was found around the bite event,  
418 raising the question of whether activity of mPFC CaMKII+ neurons is necessary for the  
419 sustained effects of ketamine during specific avoidance-related tasks. In line with our hypothesis,  
420 it is possible that activation of glutamatergic neurons is required for the initial cascade of cellular  
421 events that culminate in a long-lasting enhancement of dendritic spine number and function (2,  
422 69), while the activity of GABAergic neurons may be involved in fine-tuning these newly  
423 formed microcircuits.

424 Consistent with the involvement of GABA mechanisms in antidepressant responses, new  
425 classes of rapid-acting drugs targeting the GABA<sub>A</sub>R as positive or negative allosteric modulators  
426 (PAMs and NAMs, respectively) have emerged in recent years. Brexanolone, a positive  $\delta$ -  
427 GABA<sub>A</sub>R modulator and an analogue of the neurosteroid allopregnanolone, has recently been  
428 approved for the treatment of postpartum depression (70), marking a significant paradigm shift in  
429 the field towards identifying innovative GABAergic compounds for depression therapy.  
430 Furthermore, preclinical studies indicate that both PAMs and NAMs of the  $\alpha$ 5-containing

431 GABA<sub>A</sub>R demonstrate rapid antidepressant-like effects or prevent the behavioral responses  
432 induced by chronic stress, comparable to the effects of ketamine (71-74).

433 Therefore, enhancement of both GABA and glutamate function is likely necessary to  
434 restore signal integrity in the mPFC and other limbic regions, culminating in antidepressant  
435 states (Figure 5). Our current GABAergic evidence builds upon the findings and conceptual  
436 frameworks for antidepressant action described by Duman et al., 2019 (5) and Lusher et al., 2020  
437 (16), providing support for a sequential glutamatergic-GABAergic hypothesis for the actions of  
438 ketamine (Figure 5). While the current study provides novel insights into the GABAergic effects  
439 of ketamine, we did not evaluate causality between these mechanisms and the enhancement of  
440 glutamatergic function. Cross-correlational analyses of GABA and glutamatergic activity, as  
441 well as recordings following chemogenetic manipulation of CaMKII<sup>+</sup> neurons and ketamine  
442 treatment, would be valuable additions to investigate the temporal dynamics that could result in  
443 disinhibition. Also, further investigations are warranted to pinpoint the recruitment of specific  
444 subpopulations of GABA interneurons (e.g., SST, PV) in this biphasic response, as well as  
445 potential sex-dependent differences. In conclusion, the current findings suggest that modulating  
446 GABAergic function holds promise for developing novel antidepressant medications.

447  
448

449

450 **Author contributions**

451 M.V.F. designed the study, performed the experiments, analyzed the data and wrote the  
452 manuscript. F.D. performed experiments and provided technical support. M.R.P. provided  
453 scientific input, was involved in data interpretation and analyses, edited and revised the  
454 manuscript.

455

456 **Acknowledgements**

457 We thank Alexa-Nicole Sliby for helping for her contributions in genotyping and managing the  
458 animal colony, and Richard Crouse for his technical assistance with the photometry equipment.

459

460 **Funding**

461 This study was supported by grant MH126098, MH077681, MH105910 and NARSAD Young  
462 Investigator Award (BBRF Foundation). This work was funded in part by the State of  
463 Connecticut, Department of Mental Health and Addiction Services, but this publication does not  
464 express the views of the Department of Mental Health and Addiction Services or the State of  
465 Connecticut.

466

467 **Disclosures**

468 The authors declare that they have no conflicts of interest to report.

469

470 **Data Availability**

471 Individual subject data are shown in the figures, and any unidentified raw data will be provided  
472 upon request. MATLAB code is available at

473 [https://github.com/katemartian/Photometry\\_data\\_processing](https://github.com/katemartian/Photometry_data_processing) (34). Any additional information  
474 will be provided upon request.  
475

## 476 **References**

- 477 1. Kessler RC, Chiu WT, Demler O, Merikangas KR, Walters EE. Prevalence, severity, and  
478 comorbidity of 12-month DSM-IV disorders in the National Comorbidity Survey Replication. *Arch Gen*  
479 *Psychiatry*. 2005;62(6):617-27.
- 480 2. Duman RS, Aghajanian GK, Sanacora G, Krystal JH. Synaptic plasticity and depression: new  
481 insights from stress and rapid-acting antidepressants. *Nat Med*. 2016;22(3):238-49.
- 482 3. Trivedi MH, Rush AJ, Wisniewski SR, Nierenberg AA, Warden D, Ritz L, et al. Evaluation of  
483 outcomes with citalopram for depression using measurement-based care in STAR\*D: implications for  
484 clinical practice. *Am J Psychiatry*. 2006;163(1):28-40.
- 485 4. Berman RM, Cappiello A, Anand A, Oren DA, Heninger GR, Charney DS, et al. Antidepressant  
486 effects of ketamine in depressed patients. *Biol Psychiatry*. 2000;47(4):351-4.
- 487 5. Duman RS, Sanacora G, Krystal JH. Altered Connectivity in Depression: GABA and Glutamate  
488 Neurotransmitter Deficits and Reversal by Novel Treatments. *Neuron*. 2019;102(1):75-90.
- 489 6. Choudary PV, Molnar M, Evans SJ, Tomita H, Li JZ, Vawter MP, et al. Altered cortical  
490 glutamatergic and GABAergic signal transmission with glial involvement in depression. *Proc Natl Acad Sci*  
491 *U S A*. 2005;102(43):15653-8.
- 492 7. MacQueen GM, Yucel K, Taylor VH, Macdonald K, Joffe R. Posterior hippocampal volumes are  
493 associated with remission rates in patients with major depressive disorder. *Biol Psychiatry*.  
494 2008;64(10):880-3.
- 495 8. Csabai D, Wiborg O, Czeh B. Reduced Synapse and Axon Numbers in the Prefrontal Cortex of  
496 Rats Subjected to a Chronic Stress Model for Depression. *Front Cell Neurosci*. 2018;12:24.
- 497 9. Abdallah CG, Jackowski A, Sato JR, Mao X, Kang G, Cheema R, et al. Prefrontal cortical GABA  
498 abnormalities are associated with reduced hippocampal volume in major depressive disorder. *Eur*  
499 *Neuropsychopharmacol*. 2015;25(8):1082-90.
- 500 10. Fogaca MV, Duman RS. Cortical GABAergic Dysfunction in Stress and Depression: New Insights  
501 for Therapeutic Interventions. *Front Cell Neurosci*. 2019;13:87.
- 502 11. Duman RS, Shinohara R, Fogaca MV, Hare B. Neurobiology of rapid-acting antidepressants:  
503 convergent effects on GluA1-synaptic function. *Mol Psychiatry*. 2019.
- 504 12. Gerhard DM, Pothula S, Liu RJ, Wu M, Li XY, Girgenti MJ, et al. GABA interneurons are the  
505 cellular trigger for ketamine's rapid antidepressant actions. *J Clin Invest*. 2020;130(3):1336-49.
- 506 13. Autry AE, Adachi M, Nosyreva E, Na ES, Los MF, Cheng PF, et al. NMDA receptor blockade at rest  
507 triggers rapid behavioural antidepressant responses. *Nature*. 2011;475(7354):91-5.
- 508 14. Fogaca MV, Wu M, Li C, Li XY, Duman RS, Picciotto MR. M1 acetylcholine receptors in  
509 somatostatin interneurons contribute to GABAergic and glutamatergic plasticity in the mPFC and  
510 antidepressant-like responses. *Neuropsychopharmacology*. 2023;48(9):1277-87.
- 511 15. Singh B, Port JD, Voort JLV, Coombes BJ, Geske JR, Lanza IR, et al. A preliminary study of the  
512 association of increased anterior cingulate gamma-aminobutyric acid with remission of depression after  
513 ketamine administration. *Psychiatry Res*. 2021;301:113953.
- 514 16. Luscher B, Feng M, Jefferson SJ. Antidepressant mechanisms of ketamine: Focus on GABAergic  
515 inhibition. *Adv Pharmacol*. 2020;89:43-78.
- 516 17. Czeh B, Vardya I, Varga Z, Febbraro F, Csabai D, Martis LS, et al. Long-Term Stress Disrupts the  
517 Structural and Functional Integrity of GABAergic Neuronal Networks in the Medial Prefrontal Cortex of  
518 Rats. *Front Cell Neurosci*. 2018;12:148.
- 519 18. Godfrey KEM, Gardner AC, Kwon S, Chea W, Muthukumaraswamy SD. Differences in excitatory  
520 and inhibitory neurotransmitter levels between depressed patients and healthy controls: A systematic  
521 review and meta-analysis. *J Psychiatr Res*. 2018;105:33-44.



- 522 19. Milak MS, Proper CJ, Mulhern ST, Parter AL, Kegeles LS, Ogden RT, et al. A pilot in vivo proton  
523 magnetic resonance spectroscopy study of amino acid neurotransmitter response to ketamine  
524 treatment of major depressive disorder. *Mol Psychiatry*. 2016;21(3):320-7.
- 525 20. Ghosal S, Duman CH, Liu RJ, Wu M, Terwilliger R, Girgenti MJ, et al. Ketamine rapidly reverses  
526 stress-induced impairments in GABAergic transmission in the prefrontal cortex in male rodents.  
527 *Neurobiol Dis*. 2019:104669.
- 528 21. Sanacora G, Mason GF, Rothman DL, Behar KL, Hyder F, Petroff OA, et al. Reduced cortical  
529 gamma-aminobutyric acid levels in depressed patients determined by proton magnetic resonance  
530 spectroscopy. *Arch Gen Psychiatry*. 1999;56(11):1043-7.
- 531 22. Sanacora G, Gueorguieva R, Epperson CN, Wu YT, Appel M, Rothman DL, et al. Subtype-specific  
532 alterations of gamma-aminobutyric acid and glutamate in patients with major depression. *Arch Gen*  
533 *Psychiatry*. 2004;61(7):705-13.
- 534 23. Bhagwagar Z, Wylezinska M, Taylor M, Jezzard P, Matthews PM, Cowen PJ. Increased brain  
535 GABA concentrations following acute administration of a selective serotonin reuptake inhibitor. *Am J*  
536 *Psychiatry*. 2004;161(2):368-70.
- 537 24. Goren MZ, Kucukbrahimoglu E, Berkman K, Terzioglu B. Fluoxetine partly exerts its actions  
538 through GABA: a neurochemical evidence. *Neurochem Res*. 2007;32(9):1559-65.
- 539 25. Kucukbrahimoglu E, Saygin MZ, Caliskan M, Kaplan OK, Unsal C, Goren MZ. The change in  
540 plasma GABA, glutamine and glutamate levels in fluoxetine- or S-citalopram-treated female patients  
541 with major depression. *Eur J Clin Pharmacol*. 2009;65(6):571-7.
- 542 26. Karolewicz B, Maciag D, O'Dwyer G, Stockmeier CA, Feyissa AM, Rajkowska G. Reduced level of  
543 glutamic acid decarboxylase-67 kDa in the prefrontal cortex in major depression. *Int J*  
544 *Neuropsychopharmacol*. 2010;13(4):411-20.
- 545 27. Dubin MJ, Mao X, Banerjee S, Goodman Z, Lapidus KA, Kang G, et al. Elevated prefrontal cortex  
546 GABA in patients with major depressive disorder after TMS treatment measured with proton magnetic  
547 resonance spectroscopy. *J Psychiatry Neurosci*. 2016;41(3):E37-45.
- 548 28. Singh B, Port JD, Pazdernik V, Coombes BJ, Vande Voort JL, Frye MA. Racemic ketamine  
549 treatment attenuates anterior cingulate cortex GABA deficits among remitters in treatment-resistant  
550 depression: A pilot study. *Psychiatry Res Neuroimaging*. 2022;320:111432.
- 551 29. Wohleb ES, Wu M, Gerhard DM, Taylor SR, Picciotto MR, Alreja M, et al. GABA interneurons  
552 mediate the rapid antidepressant-like effects of scopolamine. *J Clin Invest*. 2016;126(7):2482-94.
- 553 30. Fogaca MV, Wu M, Li C, Li XY, Picciotto MR, Duman RS. Inhibition of GABA interneurons in the  
554 mPFC is sufficient and necessary for rapid antidepressant responses. *Mol Psychiatry*. 2021;26(7):3277-  
555 91.
- 556 31. Jendryka M, Palchadhuri M, Ursu D, van der Veen B, Liss B, Katzel D, et al. Pharmacokinetic and  
557 pharmacodynamic actions of clozapine-N-oxide, clozapine, and compound 21 in DREADD-based  
558 chemogenetics in mice. *Sci Rep*. 2019;9(1):4522.
- 559 32. Manvich DF, Webster KA, Foster SL, Farrell MS, Ritchie JC, Porter JH, et al. The DREADD agonist  
560 clozapine N-oxide (CNO) is reverse-metabolized to clozapine and produces clozapine-like interoceptive  
561 stimulus effects in rats and mice. *Sci Rep*. 2018;8(1):3840.
- 562 33. Pothula S, Kato T, Liu RJ, Wu M, Gerhard D, Shinohara R, et al. Cell-type specific modulation of  
563 NMDA receptors triggers antidepressant actions. *Mol Psychiatry*. 2020.
- 564 34. Martianova E, Aronson S, Proulx CD. Multi-Fiber Photometry to Record Neural Activity in Freely-  
565 Moving Animals. *J Vis Exp*. 2019(152).
- 566 35. Wei C, Han X, Weng D, Feng Q, Qi X, Li J, et al. Response dynamics of midbrain dopamine  
567 neurons and serotonin neurons to heroin, nicotine, cocaine, and MDMA. *Cell Discov*. 2018;4:60.

- 568 36. Nathanson JL, Yanagawa Y, Obata K, Callaway EM. Preferential labeling of inhibitory and  
569 excitatory cortical neurons by endogenous tropism of adeno-associated virus and lentivirus vectors.  
570 *Neuroscience*. 2009;161(2):441-50.
- 571 37. Watakabe A, Ohtsuka M, Kinoshita M, Takaji M, Isa K, Mizukami H, et al. Comparative analyses  
572 of adeno-associated viral vector serotypes 1, 2, 5, 8 and 9 in marmoset, mouse and macaque cerebral  
573 cortex. *Neurosci Res*. 2015;93:144-57.
- 574 38. Zanos P, Moaddel R, Morris PJ, Georgiou P, Fischell J, Elmer GI, et al. NMDAR inhibition-  
575 independent antidepressant actions of ketamine metabolites. *Nature*. 2016;533(7604):481-6.
- 576 39. Tremblay R, Lee S, Rudy B. GABAergic Interneurons in the Neocortex: From Cellular Properties to  
577 Circuits. *Neuron*. 2016;91(2):260-92.
- 578 40. Homayoun H, Moghaddam B. NMDA receptor hypofunction produces opposite effects on  
579 prefrontal cortex interneurons and pyramidal neurons. *J Neurosci*. 2007;27(43):11496-500.
- 580 41. Hare BD, Pothula S, DiLeone RJ, Duman RS. Ketamine increases vmPFC activity: Effects of (R)-  
581 and (S)-stereoisomers and (2R,6R)-hydroxynorketamine metabolite. *Neuropharmacology*.  
582 2020;166:107947.
- 583 42. Prescott A, Sheth C, Legarreta M, Renshaw PF, McGlade E, Yurgelun-Todd D. Altered Cortical  
584 GABA in Female Veterans with Suicidal Behavior: Sex Differences and Clinical Correlates. *Chronic Stress*  
585 (Thousand Oaks). 2018;2.
- 586 43. Kaner SJ, Colquhoun H, Doherty J, Raines S, Hoffmann E, Rubinow DR, et al. Open-label, proof-  
587 of-concept study of brexanolone in the treatment of severe postpartum depression. *Hum*  
588 *Psychopharmacol*. 2017;32(2).
- 589 44. Chowdhury GM, Zhang J, Thomas M, Banasr M, Ma X, Pittman B, et al. Transiently increased  
590 glutamate cycling in rat PFC is associated with rapid onset of antidepressant-like effects. *Mol Psychiatry*.  
591 2017;22(1):120-6.
- 592 45. Perrine SA, Ghodoussi F, Michaels MS, Sheikh IS, McKelvey G, Galloway MP. Ketamine reverses  
593 stress-induced depression-like behavior and increased GABA levels in the anterior cingulate: an 11.7 T  
594 1H-MRS study in rats. *Prog Neuropsychopharmacol Biol Psychiatry*. 2014;51:9-15.
- 595 46. Guilloux JP, Douillard-Guilloux G, Kota R, Wang X, Gardier AM, Martinowich K, et al. Molecular  
596 evidence for BDNF- and GABA-related dysfunctions in the amygdala of female subjects with major  
597 depression. *Mol Psychiatry*. 2012;17(11):1130-42.
- 598 47. Sibille E, Morris HM, Kota RS, Lewis DA. GABA-related transcripts in the dorsolateral prefrontal  
599 cortex in mood disorders. *Int J Neuropsychopharmacol*. 2011;14(6):721-34.
- 600 48. Merali Z, Du L, Hrdina P, Palkovits M, Faludi G, Poulter MO, et al. Dysregulation in the suicide  
601 brain: mRNA expression of corticotropin-releasing hormone receptors and GABA(A) receptor subunits in  
602 frontal cortical brain region. *J Neurosci*. 2004;24(6):1478-85.
- 603 49. Sequeira A, Klempan T, Canetti L, French-Mullen J, Benkelfat C, Rouleau GA, et al. Patterns of  
604 gene expression in the limbic system of suicides with and without major depression. *Mol Psychiatry*.  
605 2007;12(7):640-55.
- 606 50. Klempan TA, Sequeira A, Canetti L, Lalovic A, Ernst C, French-Mullen J, et al. Altered expression  
607 of genes involved in ATP biosynthesis and GABAergic neurotransmission in the ventral prefrontal cortex  
608 of suicides with and without major depression. *Mol Psychiatry*. 2009;14(2):175-89.
- 609 51. Luscher B, Shen Q, Sahir N. The GABAergic deficit hypothesis of major depressive disorder. *Mol*  
610 *Psychiatry*. 2011;16(4):383-406.
- 611 52. Lin LC, Sibille E. Somatostatin, neuronal vulnerability and behavioral emotionality. *Mol*  
612 *Psychiatry*. 2015;20(3):377-87.
- 613 53. Rodriguez CI, Kegeles LS, Levinson A, Ogden RT, Mao X, Milak MS, et al. In vivo effects of  
614 ketamine on glutamate-glutamine and gamma-aminobutyric acid in obsessive-compulsive disorder:  
615 Proof of concept. *Psychiatry Res*. 2015;233(2):141-7.

- 616 54. Tornese P, Sala N, Bonini D, Bonifacino T, La Via L, Milanese M, et al. Chronic mild stress induces  
617 anhedonic behavior and changes in glutamate release, BDNF trafficking and dendrite morphology only in  
618 stress vulnerable rats. The rapid restorative action of ketamine. *Neurobiol Stress*. 2019;10:100160.
- 619 55. Heinzl A, Steinke R, Poeppel TD, Grosser O, Bogerts B, Otto H, et al. S-ketamine and GABA-A-  
620 receptor interaction in humans: an exploratory study with I-123-iomazenil SPECT. *Hum*  
621 *Psychopharmacol*. 2008;23(7):549-54.
- 622 56. Wang DS, Penna A, Orser BA. Ketamine Increases the Function of gamma-Aminobutyric Acid  
623 Type A Receptors in Hippocampal and Cortical Neurons. *Anesthesiology*. 2017;126(4):666-77.
- 624 57. Rosa PB, Neis VB, Ribeiro CM, Moretti M, Rodrigues AL. Antidepressant-like effects of ascorbic  
625 acid and ketamine involve modulation of GABAA and GABAB receptors. *Pharmacol Rep*. 2016;68(5):996-  
626 1001.
- 627 58. Ren Z, Pribrag H, Jefferson SJ, Shorey M, Fuchs T, Stellwagen D, et al. Bidirectional Homeostatic  
628 Regulation of a Depression-Related Brain State by Gamma-Aminobutyric Acidergic Deficits and Ketamine  
629 Treatment. *Biol Psychiatry*. 2016;80(6):457-68.
- 630 59. Jefferson SJ, Feng M, Chon U, Guo Y, Kim Y, Luscher B. Disinhibition of somatostatin  
631 interneurons confers resilience to stress in male but not female mice. *Neurobiol Stress*. 2020;13:100238.
- 632 60. Fuchs T, Jefferson SJ, Hooper A, Yee PH, Maguire J, Luscher B. Disinhibition of somatostatin-  
633 positive GABAergic interneurons results in an anxiolytic and antidepressant-like brain state. *Mol*  
634 *Psychiatry*. 2017;22(6):920-30.
- 635 61. Du Preez A, Law T, Onorato D, Lim YM, Eiben P, Musaelyan K, et al. The type of stress matters:  
636 repeated injection and permanent social isolation stress in male mice have a differential effect on  
637 anxiety- and depressive-like behaviours, and associated biological alterations. *Transl Psychiatry*.  
638 2020;10(1):325.
- 639 62. Takatsu-Coleman AL, Patti CL, Zanin KA, Zager A, Carvalho RC, Borcoi AR, et al. Short-term social  
640 isolation induces depressive-like behaviour and reinstates the retrieval of an aversive task: mood-  
641 congruent memory in male mice? *J Psychiatry Neurosci*. 2013;38(4):259-68.
- 642 63. Agis-Balboa RC, Pinna G, Pibiri F, Kadriu B, Costa E, Guidotti A. Down-regulation of neurosteroid  
643 biosynthesis in corticolimbic circuits mediates social isolation-induced behavior in mice. *Proc Natl Acad*  
644 *Sci U S A*. 2007;104(47):18736-41.
- 645 64. Turrigiano GG, Nelson SB. Homeostatic plasticity in the developing nervous system. *Nat Rev*  
646 *Neurosci*. 2004;5(2):97-107.
- 647 65. Chiu CQ, Martenson JS, Yamazaki M, Natsume R, Sakimura K, Tomita S, et al. Input-Specific  
648 NMDAR-Dependent Potentiation of Dendritic GABAergic Inhibition. *Neuron*. 2018;97(2):368-77 e3.
- 649 66. Liang SL, Carlson GC, Coulter DA. Dynamic regulation of synaptic GABA release by the glutamate-  
650 glutamine cycle in hippocampal area CA1. *J Neurosci*. 2006;26(33):8537-48.
- 651 67. Rae C, Hare N, Bubb WA, McEwan SR, Broer A, McQuillan JA, et al. Inhibition of glutamine  
652 transport depletes glutamate and GABA neurotransmitter pools: further evidence for metabolic  
653 compartmentation. *J Neurochem*. 2003;85(2):503-14.
- 654 68. Fukumoto K, Fogaca MV, Liu RJ, Duman C, Kato T, Li XY, et al. Activity-dependent brain-derived  
655 neurotrophic factor signaling is required for the antidepressant actions of (2R,6R)-hydroxynorketamine.  
656 *Proc Natl Acad Sci U S A*. 2019;116(1):297-302.
- 657 69. Li N, Lee B, Liu RJ, Banasr M, Dwyer JM, Iwata M, et al. mTOR-dependent synapse formation  
658 underlies the rapid antidepressant effects of NMDA antagonists. *Science*. 2010;329(5994):959-64.
- 659 70. Morrow AL, Balan I, Boero G. Mechanisms Underlying Recovery From Postpartum Depression  
660 Following Brexanolone Therapy. *Biol Psychiatry*. 2022;91(3):252-3.
- 661 71. Troppoli TA, Zanos P, Georgiou P, Gould TD, Rudolph U, Thompson SM. Negative Allosteric  
662 Modulation of Gamma-Aminobutyric Acid A Receptors at alpha5 Subunit-Containing Benzodiazepine

663 Sites Reverses Stress-Induced Anhedonia and Weakened Synaptic Function in Mice. *Biol Psychiatry*.  
664 2022;92(3):216-26.  
665 72. Xiong Z, Zhang K, Ishima T, Ren Q, Chang L, Chen J, et al. Comparison of rapid and long-lasting  
666 antidepressant effects of negative modulators of alpha5-containing GABAA receptors and (R)ketamine in  
667 a chronic social defeat stress model. *Pharmacol Biochem Behav*. 2018;175:139-45.  
668 73. Piantadosi SC, French BJ, Poe MM, Timic T, Markovic BD, Pabba M, et al. Sex-Dependent Anti-  
669 Stress Effect of an alpha5 Subunit Containing GABAA Receptor Positive Allosteric Modulator. *Front*  
670 *Pharmacol*. 2016;7:446.  
671 74. Zanos P, Nelson ME, Highland JN, Krimmel SR, Georgiou P, Gould TD, et al. A Negative Allosteric  
672 Modulator for alpha5 Subunit-Containing GABA Receptors Exerts a Rapid and Persistent Antidepressant-  
673 Like Action without the Side Effects of the NMDA Receptor Antagonist Ketamine in Mice. *eNeuro*.  
674 2017;4(1).  
675

676 **Figure legends**

677 **Figure 1. Photometry recordings from mPFC glutamatergic and GABAergic neurons**  
678 **immediately after ketamine treatment.** (A) Time course for surgery, treatment and recording.  
679 (B) Representative images of the mPFC from *Gad1-Cre* mice showing unilateral infusion of  
680 CaMKII-driven GCaMP6s (CaMKII-GCaMP6s) and Cre-dependent jRCaMP1b (Gad-RCaMP)  
681 virus, labeling pyramidal and GABAergic cells, respectively, along with implantation of an  
682 optical fiber (magnification: 10X). (C) Ketamine increased calcium transients in glutamatergic  
683 neurons (CaMKII+) compared to both the baseline (BL, - 20 to 0 min) and vehicle-treated  
684 animals 30 min post-treatment, persisting until the end of the recording session ( $F_{\text{treatment } 1,8} =$   
685  $22.03$ ;  $F_{\text{interaction } 4,32} = 4.99$ ,  $p \leq 0.05$ ). (D) Ketamine produced a biphasic response in GABA  
686 neuron calcium activity, in which there was an initial decrease (0 to 30 min) followed by an  
687 increase in the photometry signal (60 to 120 min) ( $F_{\text{time } 4,32} = 5.23$ ;  $F_{\text{interaction } 4,32} = 9.65$ ,  $p \leq 0.05$ ).  
688 (E) Ketamine increased excitation/inhibition (E/I) levels within 10 min of administration, which  
689 returned to baseline levels shortly thereafter ( $F_{\text{treatment } 1,8} = 27.43$ ;  $F_{\text{interaction } 2,16} = 6.22$ ,  $p \leq 0.05$ ).  
690 (F) Minimally processed traces representing pyramidal neurons (CaMKII+) expressing  
691 GCaMP6s and (G) GABA neurons (Gad-Cre) expressing RCaMP in the mPFC from a vehicle-  
692 or ketamine-treated *Gad1-Cre* mouse. The black arrow indicates the treatment time. Horizontal  
693 dashed lines indicate  $z \text{ dF/F} = 0$ . Photometry results per animal are computed as average z-scored  
694 dF/F, and graphs are presented as mean  $\pm$  standard error. Repeated measures ANOVA followed  
695 by Sidak correction for multiple analysis; \* $p \leq 0.05$  in comparison to the vehicle-treated group;  
696 # $p \leq 0.05$  in comparison to the baseline (before treatment),  $n = 10/\text{group}$ .  $F_{\text{interaction}}$  represents the  
697 interaction between time and treatment factors.

698

699 **Figure 2. Photometry recordings from glutamatergic and GABAergic neurons 24 h after**  
700 **ketamine treatment and during the sucrose splash test.** (A) Timeline for surgery, treatment,  
701 recording and behavioral testing. (B) Ketamine increased the grooming time in the sucrose  
702 splash test (SUST) 24 h after administration ( $t_{16} = 3.01$ ,  $p \leq 0.05$ ). (C-E) No change in baseline  
703 (BL, -300 to 0 sec) activity of pyramidal or GABA neurons was observed 24 h after ketamine  
704 administration ( $p > 0.05$ ). (C) There was an enhancement of calcium transients in both pyramidal  
705 ( $F_{\text{time } 1,8} = 25.16$ ;  $F_{\text{interaction } 1,8} = 6.51$ ,  $p \leq 0.05$ ) and (D) GABA neurons ( $F_{\text{time } 1,8} = 9.63$ ;  $F_{\text{interaction}}$   
706  $_{1,8} = 24.86$ ,  $p \leq 0.05$ ) in ketamine-treated animals during the SUST (0 to 300 sec) compared to  
707 both the baseline and vehicle groups. (E) 60-sec binned representation of the grooming time  
708 (orange), GCaMP6s (green,  $z$  dF/F) and RCaMP (red,  $z$  dF/F) during the SUST duration. (F)  
709 Representative traces of pyramidal neurons (CaMKII+) expressing GCaMP6s and (G) GABA  
710 neurons (Gad-Cre) expressing RCaMP in the mPFC from vehicle- and ketamine-treated *Gad1-*  
711 *Cre* mice before and during the SUST. Photometry results per animal are computed as average  $z$ -  
712 scored dF/F, and graphs are presented as mean  $\pm$  standard error. Repeated measures ANOVA  
713 followed by Sidak correction for multiple analysis; \* $p \leq 0.05$  in comparison to the vehicle-  
714 treated group; # $p \leq 0.05$  in comparison to the baseline (before test),  $n = 9/\text{group}$ .  $F_{\text{interaction}}$   
715 represents the interaction between time and treatment factors.

716

717 **Figure 3. Photometry recordings from glutamatergic and GABAergic neurons 72 h after**  
718 **ketamine treatment and during the novelty suppressed feeding test.** (A) Timeline for  
719 surgery, treatment, recording and behavioral testing. (B) Ketamine decreased the latency to feed  
720 in the novelty suppressed feeding test (NSFT) 72 h after administration ( $U = 16$ ,  $p \leq 0.05$ ). (C)  
721 Ketamine did not change baseline (BL, -300 to 0 sec) activity of pyramidal cells 72 h after

722 administration ( $p > 0.05$ ) and produced a trend towards increased pyramidal activity during the  
723 NSFT (150-sec time blocks; vehicle:  $\chi^2_{(4)} = 2.22$ ,  $p > 0.05$ ; ketamine:  $\chi^2_{(4)} = 9.24$ ,  $p = 0.06$ ). (D)  
724 No change was observed during the bite event ( $t_{16} = 0.19$ ,  $p > 0.05$ ). (E) Representative traces of  
725 pyramidal neurons (CaMKII+) expressing GCaMP6s in the mPFC from vehicle- and ketamine-  
726 treated *Gad1-Cre* mice before and during the NSFT. (F) Ketamine did not change baseline  
727 activity of GABA neurons 72 h after administration (-300 to 0 sec,  $p > 0.05$ ). However, exposure  
728 to the NSFT resulted in an enhancement of GABA neuron activity in both vehicle- and  
729 ketamine-treated groups ( $F_{\text{time } 4,32} = 58.83$ ;  $F_{\text{interaction } 4,32} = 3.23$ ,  $p \leq 0.05$ ), with a more robust  
730 activity observed in the ketamine- compared to the vehicle-group in the first 150 sec of the test  
731 (0-150 sec,  $p \leq 0.05$ ). (G). Ketamine increased calcium activity in GABA neurons during the bite  
732 event ( $t_{16} = 2.45$ ,  $p \leq 0.05$ ). (H) Representative traces of GABA neurons (*Gad-Cre*) expressing  
733 RCaMP in the mPFC from vehicle- and ketamine-treated *Gad1-Cre* mice before and during the  
734 NSFT. Black arrows represent a bite event. Photometry results per animal are computed as  
735 average z-scored dF/F and graphs are presented as mean  $\pm$  standard error. Repeated measures  
736 ANOVA followed by Sidak correction for multiple analysis, Friedman's two way analysis of  
737 variance by ranks or Mann-Whitney U test; \* $p \leq 0.05$  in comparison to the vehicle-treated group;  
738 # $p \leq 0.05$  in comparison to the baseline (before test),  $n = 9/\text{group}$ .  $F_{\text{interaction}}$  represents the  
739 interaction between time and treatment factors.

740

741 **Figure 4. GABA neuron activity is necessary for the sustained behavioral actions of**  
742 **ketamine.** (A) Timeline for surgery, treatments, and behavioral testing. (B) Representative  
743 images of the mPFC from *Gad1-Cre* and WT (Cre-negative littermate) mice that received  
744 bilateral infusions of hM4DGi virus (magnification: 10X; inset: 60X). (C) Co-labeling

745 percentage of PV or SST cells with hm4DGi virus in mPFC sections from *Gad-Cre* mice  
746 (magnification: 20X; inset: 40X). (D) CNO administration 40 min (1 mg/kg) and 2 h (0.5 mg/kg)  
747 post-ketamine treatment blocked its behavioral effects in the sucrose splash test (SUST, 24 h  
748 post-ketamine;  $F_{\text{genotype } 1,3} = 13.42$ ,  $F_{\text{treatment } 1,3} = 6.33$ ,  $F_{\text{interaction } 1,3} = 14.52$ ,  $p \leq 0.05$ ) and (E)  
749 novelty suppressed feeding test (NSFT, 72 h post-ketamine;  $F_{\text{interaction } 1,3} = 4.67$ ,  $p \leq 0.05$ ). There  
750 was no change in home cage food consumption ( $F_{\text{interaction } 1,3} = 0.22$ ,  $p > 0.05$ ). (F) Timeline for  
751 surgery, treatments, and behavioral testing. (G) CNO administration (1 mg/kg) 30 min before the  
752 behavioral test occluded the behavioral effects of ketamine in the sucrose splash test (SUST, 24 h  
753 post-ketamine;  $F_{\text{treatment } 1,3} = 4.34$ ,  $F_{\text{interaction } 1,3} = 4.21$ ,  $p \leq 0.05$ ) and (H) novelty suppressed  
754 feeding test (NSFT, 72 h post-ketamine;  $F_{\text{interaction } 1,3} = 4.66$ ,  $p \leq 0.05$ ). There was no change in  
755 home cage food consumption ( $F_{\text{interaction } 1,3} = 0.30$ ,  $p > 0.05$ ). Graphs are presented as mean  $\pm$   
756 standard error. Two-way ANOVA followed by Duncan; \* $p < 0.05$  in comparison to the WT  
757 vehicle-treated group; # $p < 0.05$  in comparison to the WT ketamine-treated group.  $F_{\text{interaction}}$   
758 represents the interaction between genotype and treatment factors.

759

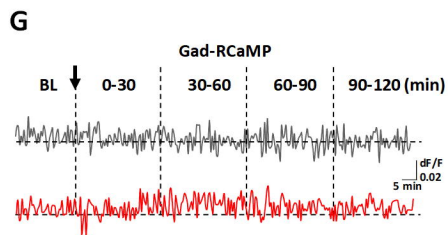
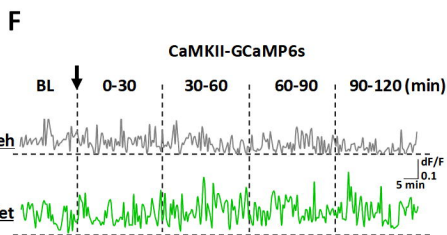
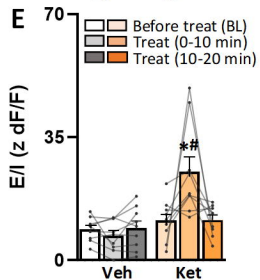
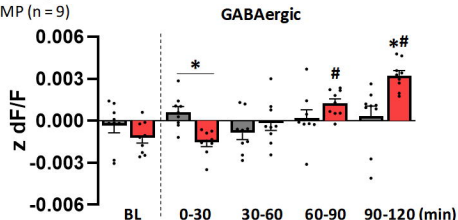
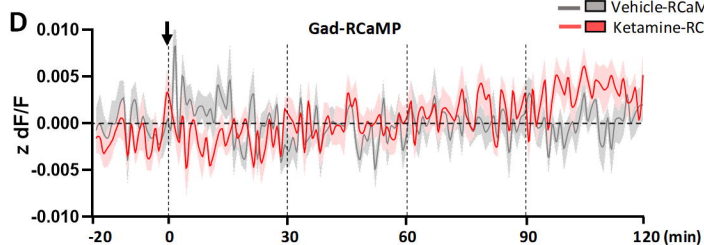
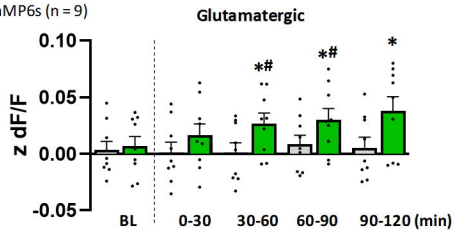
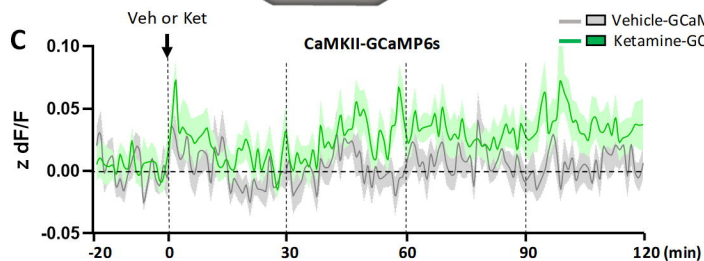
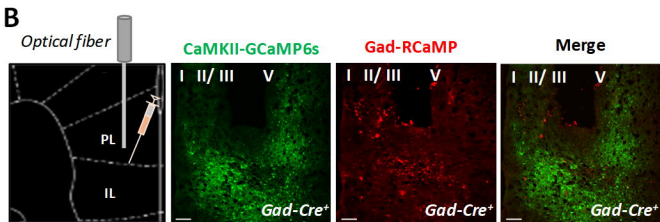
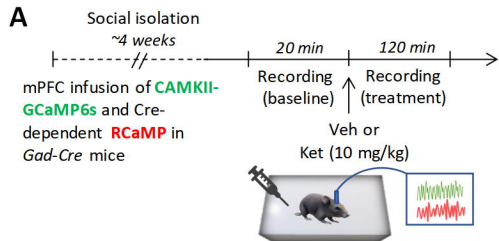
760 **Figure 5. Biphasic glutamatergic-GABAergic model for ketamine action.** (A) Major  
761 depressive disorder (MDD) and chronic stress impair glutamate and GABA function in the  
762 mPFC, leading to altered connectivity and network dysfunction in corticolimbic brain regions, as  
763 suggested by previous studies (5, 14, 18, 20, 60, 69). (B) Ketamine restores these deficits by  
764 acting through two phases: (1a) In phase 1 (acute), ketamine blocks the activity of GABA  
765 interneurons via NMDA-R, disinhibiting pyramidal cells and generating a glutamate burst and  
766 increasing excitation/inhibition (E/I) levels (1b). The glutamate burst triggers a cascade of  
767 cellular events culminating in synaptic plasticity and fast antidepressant responses, as suggested

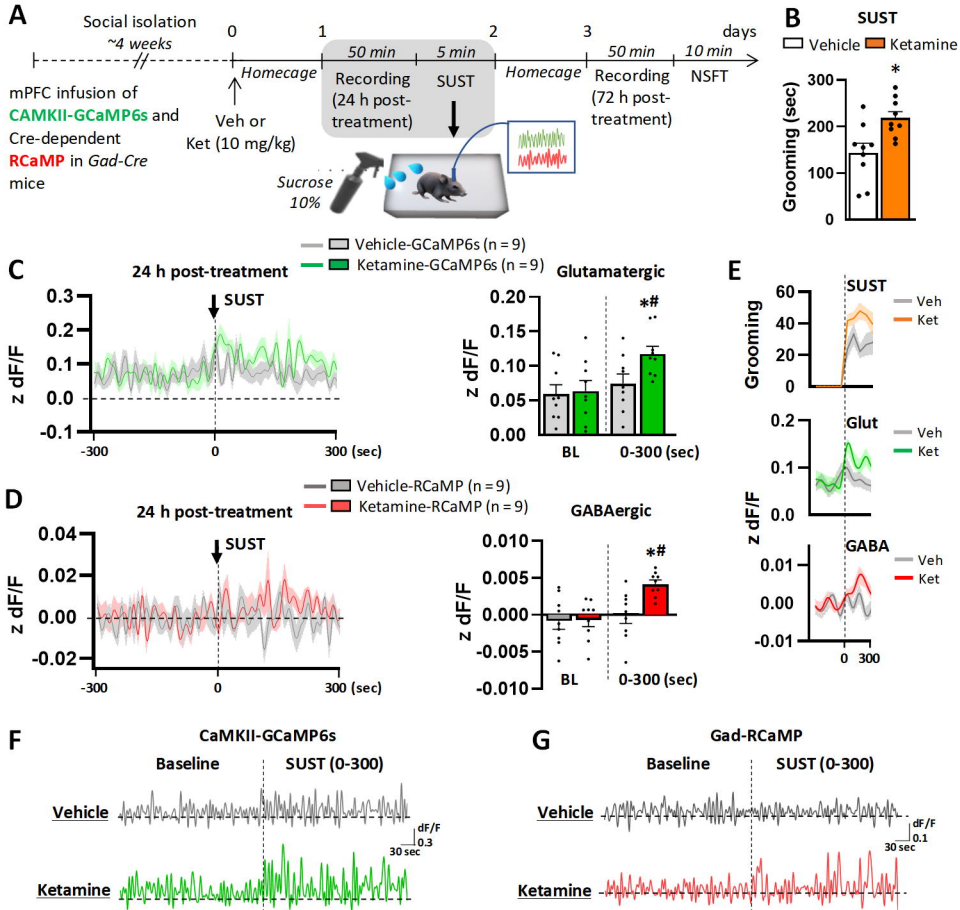


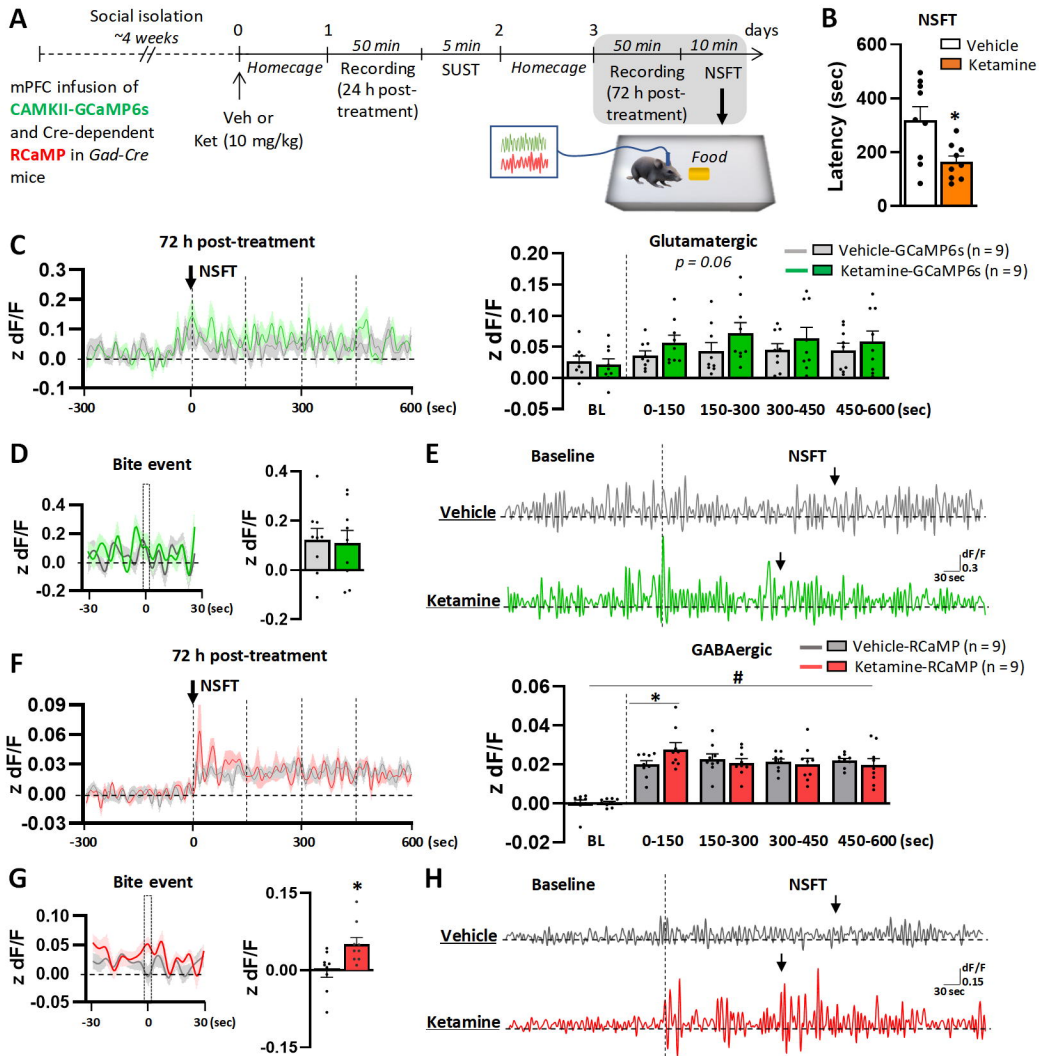
768 by previous studies (12, 20, 30, 69). In a second phase (sustained), there is a self-tuning  
769 adjustment to reach E/I balance in the mPFC, leading to potentiation of GABAergic function  
770 (2a) and restored circuit connectivity (2b). The recruitment of long-lasting increases in GABA  
771 neuron activity contributes to sustained antidepressant effects. Created with BioRender.com.

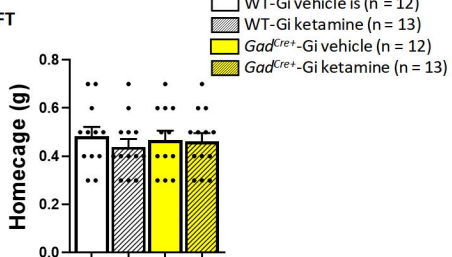
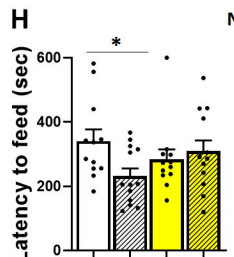
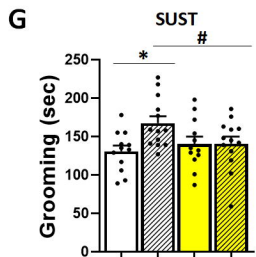
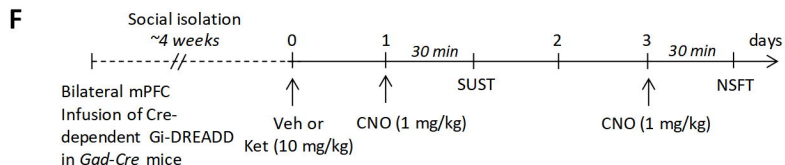
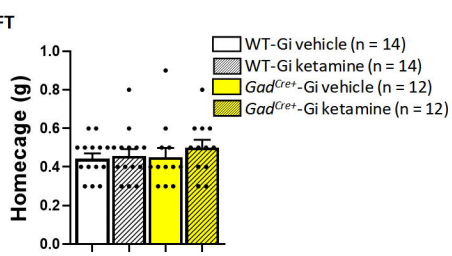
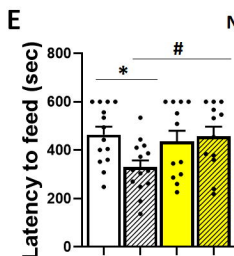
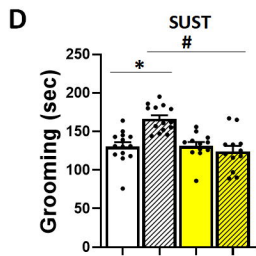
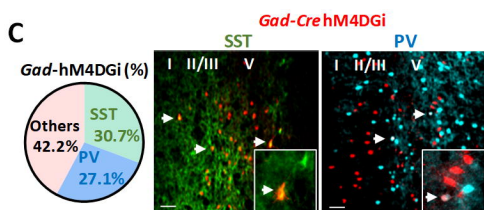
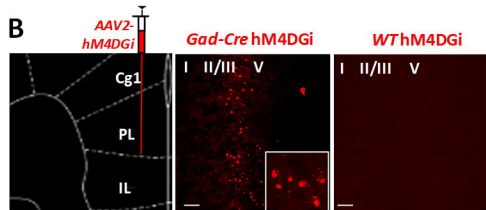
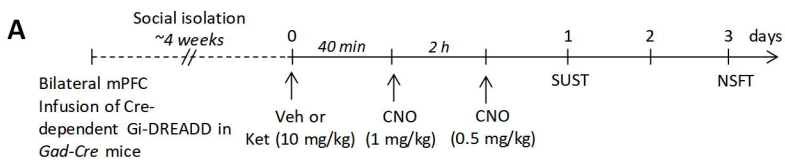
772

773



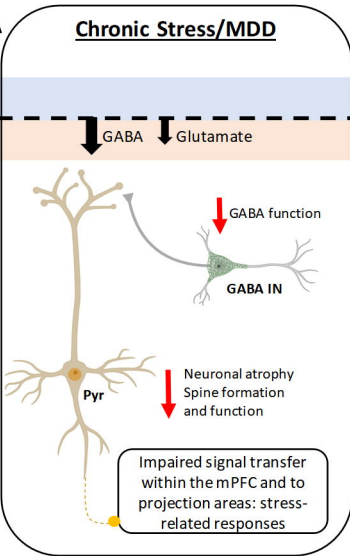






# A Chronic Stress/MDD

Adaptive state  
Homeostasis  
Disease state



# B Rapid antidepressants

Phase 1 (rapid)

Phase 2 (sustained)

